The Thermal Behavior Analysis in Tap-Hole Area

YUNG-CHANG KO*, CHUNG-KEN HO* and HSU-TANG KUO**

**Department of Steel and Aluminum Research and Development*
***Blast Furnace Plant-I, Department of Irommaking*
China Steel Corporation
Hsiao Kang, Kaohsiung 81233, Taiwan, R.O.C.

The No. 2 blast furnace at China Steel Corporation (CSC) had a splashing problem from its new campaign in January 2006. It was inferred that the splashing was somehow related to the performance of the refractory and cooling system near the tap-hole area. This study establishes a blast furnace hearth model to investigate the thermal behavior in terms of refractory and mud, in the tap-hole area, by using a CFD code Fluent. The accuracy of the model was verified by comparing the simulated temperature distribution with site practical data. Based on the numerical simulation, it is found that the thermal properties of mud-core, castable and brick and the convection heat transfer coefficient of spool have a significant effect on the tap-hole area temperature distribution. The developed hearth model can predict the trend of thermal behavior by adjusting material thermal properties and is helpful in understanding the temperature distribution of the tap-hole area, which can be a reference to adjust the cooling operation.

1. INTRODUCTION

Many works about the hearth phenomena of blast furnace, such as molten iron flow, mass and heat transfer, have been done. These mathematical models give a basic understanding about molten iron flow and the heat transfer in the blast furnace hearth, while only a few focuses on the tap-hole area. Vats and dash[(1)] computed the wall shear stress by solving the flow field and concluded that there exists an optimal tap-hole length for minimal wall shear stress, which has also been verified in their present work. However, their model did not consider various possible coke-bed positions and shapes, nor the model did not show experimental validation. Dash et al[(2-3)] discussed the optimal tap-hole angle for minimal flow－－induced shear stress on the wall of the blast furnace hearth, but their study only concentrated on a fixed coke-bed size and shape.

Excessive splashing of a hot metal stream from tap-hole, which is caused by entrained blast air, can result in premature trough refractory wear. This splash occurs when the gas-liquid flow regime of slug flow is present in the tap-hole. Tap-hole stream trajectories and their effects on trough refractory, reported by He et al,[(4)] can be predicted by the theory proposed herein that recognizes that the average velocity in the liquid stream is equal to the sum of the gas and liquid superficial velocities.

After more than 12 years in operation, No. 2 blast furnace of China Steel Corporation (CSC) was blown down in October 2005 for revamping, and its 3rd campaign begun in January 2006. During the revamping, the furnace hearth was equipped with stave cooling instead of shell water spray cooling. This is the first time one of one of CSC's blast furnaces has used stave cooling in the hearth. Unfortunately, splashy tap-hole streams occurred very frequently and severely in the beginning of casting in this blast furnace. It was inferred that the splashing was somehow related to the performance of the refractory and cooling system near tap-hole area. This study establishes a blast furnace hearth model to investigate the thermal behavior in terms of refractory and mud in tap-hole area, by using a CFD code Fluent.

2. PHYSICAL SYSTEM

In order to save computing time, a 2-D model was used to investigate the effect of the thermal properties and cooling parameters. Figure 1 shows a schematic diagram of the No. 2 blast furnace hearth, in X-Y plane. In the hearth side wall, copper staves were installed in the area of the tap-holes, and cast iron staves were used in the rest of the area. Besides, water-cooling steel pipes were arranged in the hearth bottom. Then, a 3-D simplified model was also developed to simulate the temperature distribution in the tap-hole area, as is illustrated in Fig. 2. As we focused on the tap-hole temperature profile, only hot metal in the tap-hole was

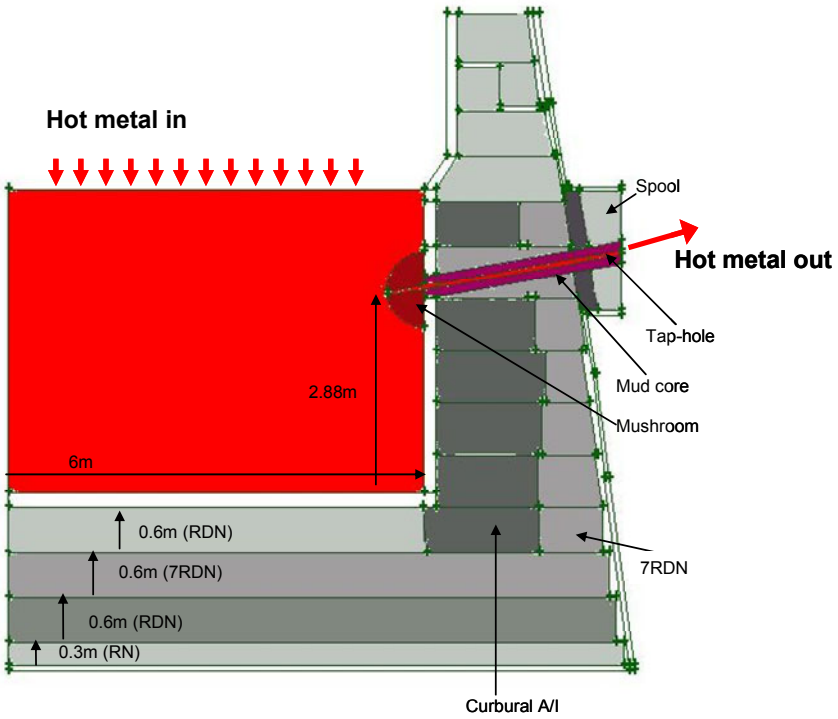

Fig. 1. 2-D Geometric dimensions and refractory components of hearth.

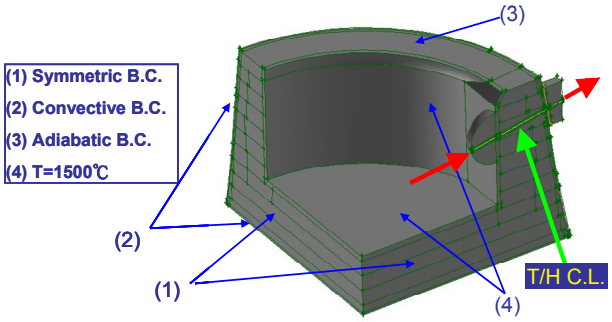

Fig. 2. 3-D model of hearth and boundary conditions.

considered. The hearth wall temperature was set as a constant temperature, 1500°C. The model parameters are listed in Table 1.

3. GOVERNING EQUATIONS AND NUMERICAL METHOD

3.1 Governing Equations

Based on the previous work,[5] the Navier-Stoke equations with conjugate heat transfer were solved to generate the hot metal flow field in the hearth and the heat flux across the side wall and the bottom. The governing equations for this conjugate heat transfer problem can be described as follows:

Table 1 Standard Values of Model Parameters

Iron	
Laminar viscosity	0.00715 Pa s
Thermal conductivity	16.5 W m^{-1} k^{-1}
Heat capacity	850 J kg^{-1} k^{-1}
Density	7000 kg m^{-3}
Refractories	
Thermal conductivity of Protection Wall	2.6 W m^{-1} k^{-1}
Thermal conductivity of RN	150 W m^{-1} k^{-1}
Thermal conductivity of RD-N	11 W m^{-1} k^{-1}
Thermal conductivity of Carbural A/l	7 W m^{-1} k^{-1} (T=473.15K); 8 W m^{-1} k^{-1} (T=673K); 10 W m^{-1} k^{-1} (T=873K); 11 W m^{-1} k^{-1} (T=1073K)
Thermal conductivity of 7 RD-N	16 W m^{-1} k^{-1} (T<473K) ; 18 W m^{-1} k^{-1} (T>1373K)
Thermal conductivity of Copper Stave	388.68 W m^{-1} k^{-1}
Thermal conductivity of Cast-iron Stave	50.079 W m^{-1} k^{-1}
Coke bed	
Particle diameter	0.03 m
Porosity	0.35
Boundary condition	
Convection coefficient	3000 w m^{-2} k^{-1}

$$\frac{\partial \rho U_i}{\partial x_i} = 0 \quad \text{.....(1)}$$

$$\frac{\partial \rho U_i U_j}{\partial x_j} = -\frac{\partial p}{\partial x_i} + \frac{\partial}{\partial x_i}\left[\mu\left\{\frac{\partial U_i}{\partial x_j} + \frac{\partial U_j}{\partial x_i}\right\}\right] + \rho g_i \text{ ..(2)}$$

$$\rho C_p U_i \frac{\partial T}{\partial x_i} = k\frac{\partial^2 T}{\partial x_i^2} \quad \text{.....(3)}$$

$$S_m = -\frac{\mu}{\alpha} U_i \quad \text{.....(4)}$$

$$\alpha = \frac{D_p^2 \varepsilon^3}{150(1-\varepsilon)^2} \quad \text{.....(5)}$$

Where
U is the velocity of hot metal (m/s)
ρ is the density of hot metal (kg/m^3)
g is the gravitational acceleration (m/s^2)
C_p is the heat capacity (J/kg-K)
T is the temperature (K)
k is the thermal conductivity (W/m-K)
α is defined as the permeability (-)
D_p is the coke mean diameter (m)
ε is porosity (-), and
S_m is the momentum source term caused by the deadman (Pa/m).

To obtain S_m, the deadman was modelled as a porous media, and Darcy's Law, simplified from Ergun equation and shown in Equation 6 for the 2-D model, was adopted to address the pressure drop in terms of kinetic energy and viscous energy losses.

$$\frac{|\Delta p|}{L} = \frac{150\mu(1-\varepsilon)^2}{D_p^2 \varepsilon^3} \upsilon + \frac{1.75(1-\varepsilon)}{D_p \varepsilon^3} \rho \upsilon^2 \quad \text{.....(6)}$$

where
p is pressure (N/m^2)
L is the characteristic length (m)
υ is the superficial velocity (m/s).

3.2 Assumptions and Boundary Conditions

Base case assumptions made for this study included the following:

(1) The drainage process is steady state, so the hot metal flows in and out at a constant rate; after mud-plugging, the process is unsteady state and the sintered mud temperature varies with time.
(2) Chemical reactions are ignored;
(3) The hearth lining is kept intact in the beginning of campaign;
(4) Only force convection and heat conduction are considered for the heat transfer between the hot metal and refractory ;[5]
(5) Turbulence influence is neglected;

The following boundary conditions were imposed for all cases:

(1) The hot metal level is constant in the 2-D model, and only hot metal in the tap-hole is considered in the 3-D model;
(2) The free surface of hot metal is defined as an inlet flow boundary, in which the hot metal of 1,500°C is uniformly distributed into the hearth in 2-D model and the hearth wall temperature is defined as a constant temperature, 1,500°C;
(3) The convectional heat transfer in the hearth outside surface is set according to the convective coefficient between stave and cooling water;
(4) The taphole exit is kept at atmospheric pressure, and a mass flow boundary condition is implemented to ensure mass balance;
(5) The refractory in the free surface level is adiabatic;
(6) A symmetrical wall boundary is used through the vertical axis of the hearth center; and
(7) At hearth side and bottom wall surface, no-slip boundary conditions are employed.

4. NUMERICAL PROCEDURE

The set of governing equations (1)-(5) were discretized using the finite volume technique in a computational domain and can be solved numerically. The discreterization of the momentum and continuity equations and their solutions were solved by means of the segregated solver. A standard pressure interpolation scheme was required to compute the face values of pressure from the cell values. SIMPLE algorithm was applied in pressure-velocity coupling in the segregated solver to adjust the velocity fields by correcting the pressure field. The second upwind scheme was chosen to discrete the convection term of every governing equation. As displayed in Figs 1 and 2, the steady state analytical domain included the hot-metal region and refractory. For numerical procedure, the temperature distribution during drainage was calculated first. Then, the unsteady state model is proposed to calculate the temperature variation with time in the tap-hole.

5. RESULTS AND DISCUSSIONS

5.1 Temperature Distribution During Tapping and Mud Plugging

To investigate the temperature distribution of the hearth, a temperature profile was computed by a 2-D blast furnace model. Figure 3 shows a general case of 2-D temperature distribution of the hearth during tapping and mud-plugging. The effect of mud sintered time on temperature after plugging is not remarkable at the hearth bottom. The main difference in Fig. 3 was

the heat concentration in the tap-hole area due to adiabatic refractory installed between the carbon brick and castable. After plugging, the mud was heated first to maximum temperature, then cooled by the refractory around tap-hole and cooling system. Therefore, the temperature distribution near the tap-hole is more remarkable with time.

5.2 Sensibility Analysis of Refractory'S Thermal Properties

5.2.1 Temperature Distribution in Tap-Hole

Different tapping sequences, such as alternate tapping, mother and daughter tapping and one side tapping, were used in the mill to prevent splashing. The effect of the different tapping sequences was investigated by adopting a tap-hole temperature measurement, with tap-hole were measurements being taken at 20 minute, 60 minute and 120 minute after mud plugging. The measured temperature profile is shown in Fig. 4.

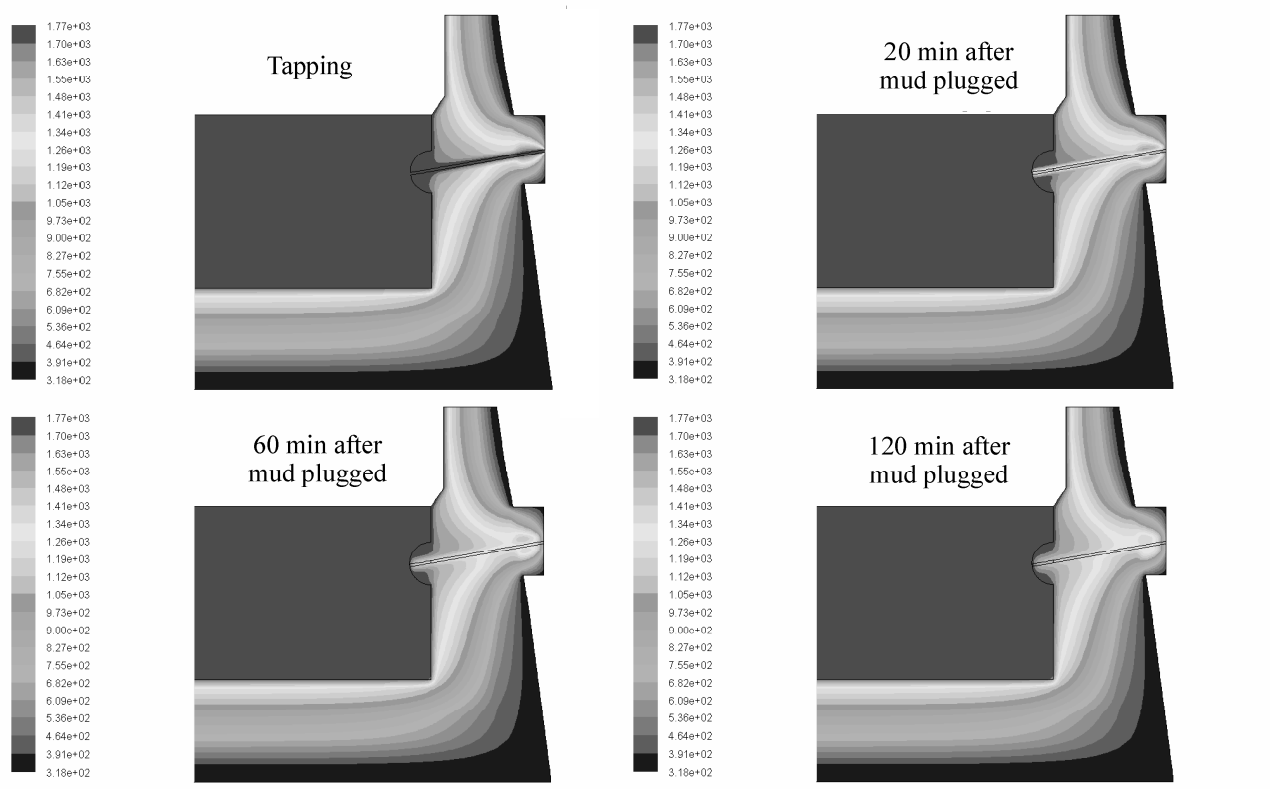

Fig. 3. Temperature contours of hearth with different time.

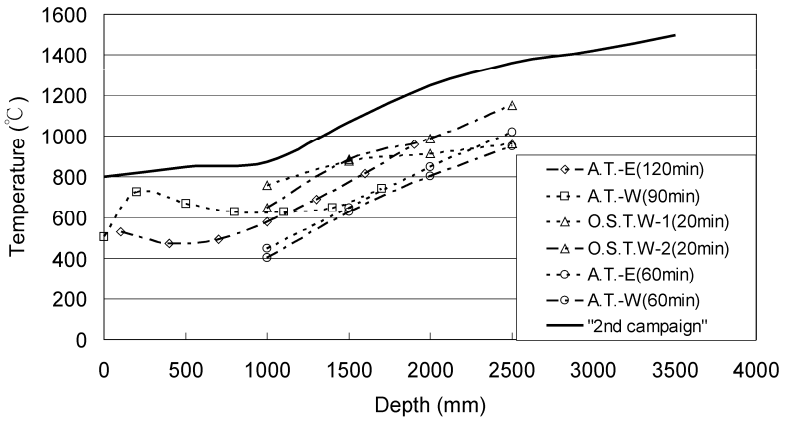

Fig. 4. Measured temperature in tap-hole of No. 2 blast furnace of CSC.

The temperature profile of one side tapping was higher than the one of alternate tapping due to shorter cooling time. Comparing to the measured temperatures of the last campaign, the tap-hole temperatures of the new campaign were too low to sinter the mud. This could be the main reason of splashing. Since the tap-hole temperature can not measured all the time, a mathematic model was used to simulate the tap-hole temperature profile in this study in order to find the main influence of the refractory and cooling system on the tap-hole temperature distribution.

5.2.2 Effect of Surface Convective Condition

Figure 5 shows the effect of the surface heat transfer properties of cooling condition on tap-hole temperature distribution. The effect of water cooling on the stave, with the heat convective coefficient (h) assumed to be 300 and 3,000 $wm^{-2}k^{-1}$, are shown in Fig. 5(a). The effect of air cooling on the spool surface, an adopted with convective coefficient of 30 and 300 $wm^{-2}k^{-1}$, are shown in Fig. 5(b). The major effect in the tap-hole area of the convective coefficient was on the temperature of the spool surface. A higher convective coefficient causes a lower surface temperature of the spool. Both of convective coefficients have slight influence in the tap-hole temperature distribution.

5.2.3 Effect of Thermal Property of Refractory

The different thermal conductivities of mud, high alumina brick and castable are adopted to investigate the effect of the thermal conductivity of the refractory, as shown in Fig. 6. The case with mud-core around the tap-hole was computed. The influence of the thermal conductivity of mud was found not to be remarkable due to the small volume. The temperature profile of the tap-hole has a peak value in the spool area due to the lower thermal conductivity of high alumina brick and castable. These adiabatic materials induce heat

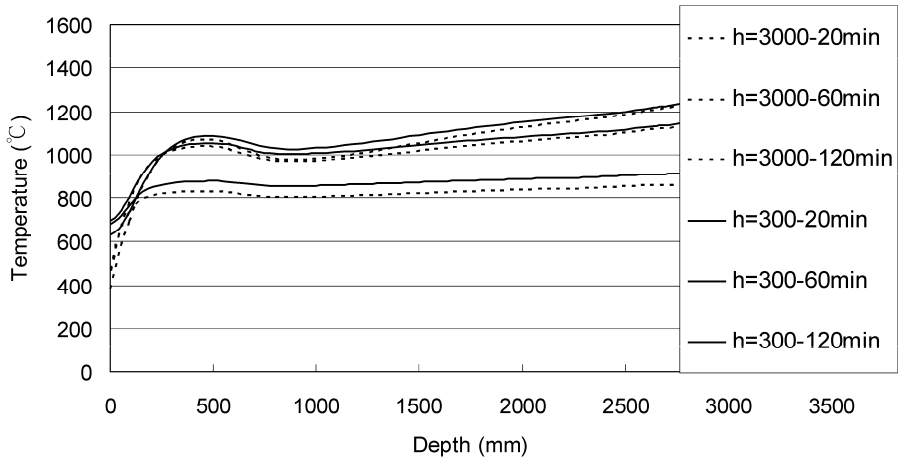

(a) Convective coefficient of water in stave

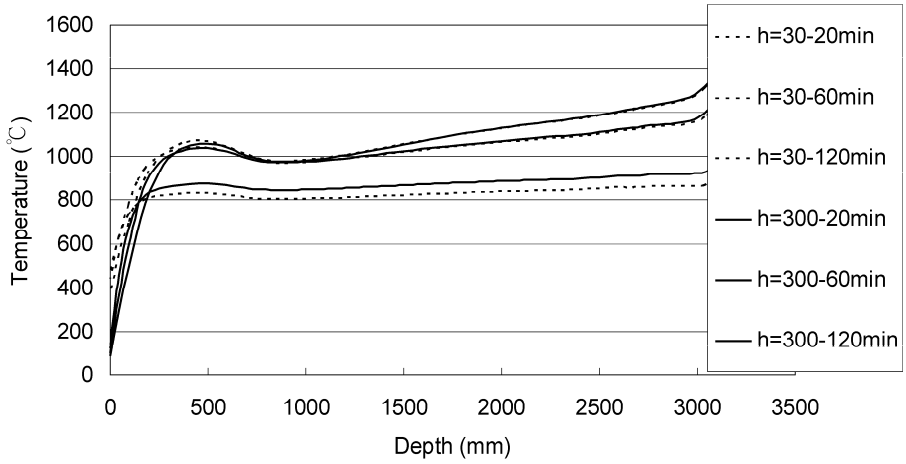

(b) Convective coefficient of spool surface

Fig. 5. The effect of surface heat transfer properties of cooling conditions on tap-hole temperature distribution.

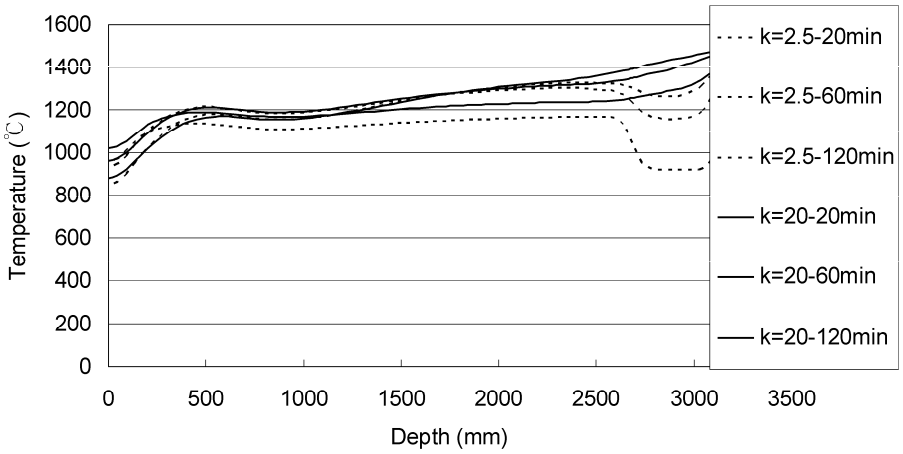

(a) Thermal conductivity of mud

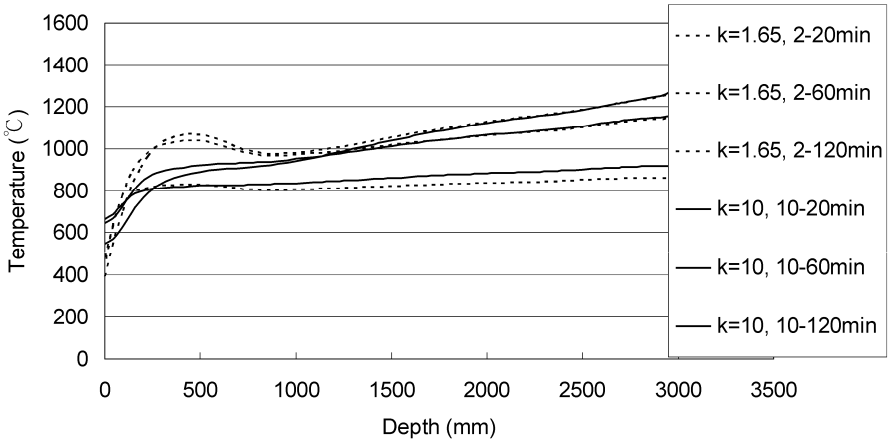

(b) Thermal conductivity of high Al_2O_3 brick and castable

Fig. 6. The effect of thermal properties of refractories on tap-hole temperature distribution.

concentration in spool. In Fig. 7 shows the effect of mud-core with lower thermal conductivity. In this study, the thermal conductivity of the mud-core was 5 $Wm^{-1}k^{-1}$, which is between the conductivity of mud and hot metal. The lower conductivity means that the heat flux into mud is harder and causes a lower temperature profile than the mud-core. Actually, the mud-core is a mixed layer containing mud, iron, slag and cracked brick. Therefore, the thermal conductivity of this layer is hard to define and control.

5.3 Effect of 2-D and 3-D Model Simulation

According to the sensibility analysis, it can be found that the thermal conductivity of the mud-core plays an important role in tap-hole temperature distribution. We tried to simulate tap-hole temperature with effective resistance in the spool area. Figure 8 shows the temperature profiles of the tap-hole by 2-D simulation and by measurement. The measured temperature profile is higher than the simulated one, and the slope is steeper than the simulated one. This is due to the limitation of the 2-D model. For a hearth model with a spool area, it is not an axial symmetry problem and is hard to simulate. Therefore, the studies regarding the spool area of the hearth were simplified in general, even in the 3-D model. Trying to better simulate the tap-hole temperature, a simplified 3-D model was adopted and is shown in Fig. 2. Figure 9 shows the temperature profiles simulated in the 3-D model with values of the base parameters shown in Table 1. The simulation result can get good agreement with measured data. A simplified 3-D model can simulate the tap-hole temperature profile. Making a comparison between Fig. 4 and Fig. 9, it is clear that the temperature profile of the tap-hole is too low to sinter mud well and could cause splashing. Therefore, the model can provide some information to site personnel for dealing with hot metal splashing and the selection of new mud for the tap-hole.

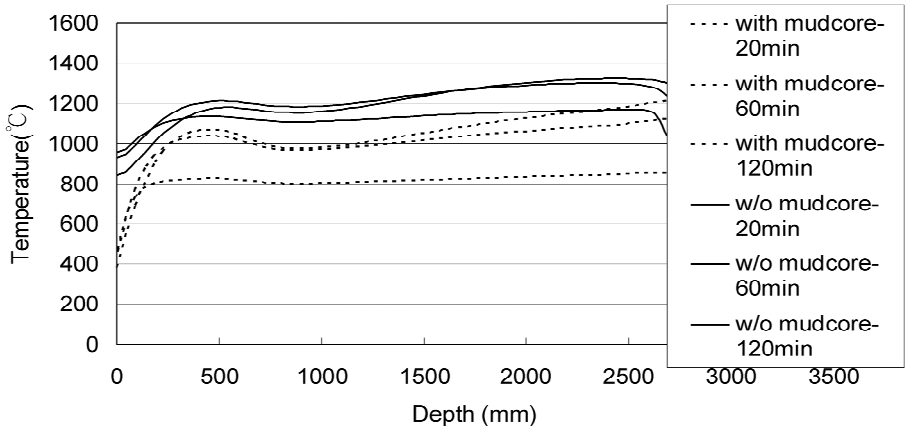

Fig. 7. The effect of mud-core on tap-hole temperature distribution..

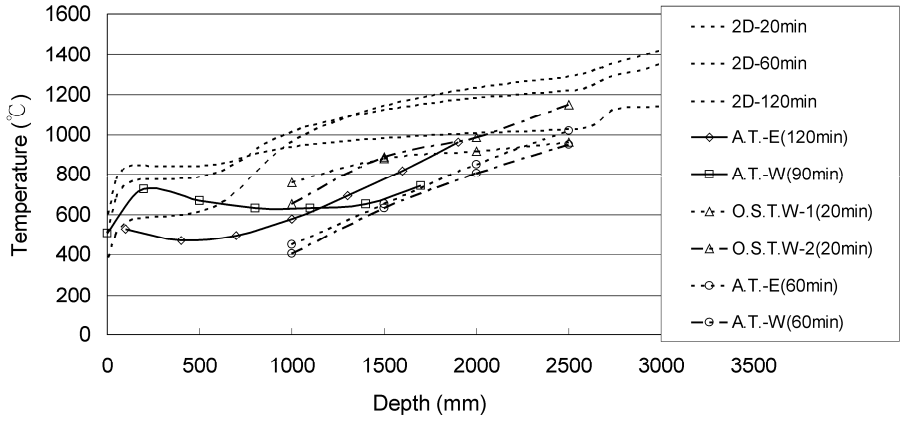

Fig. 8. Measured temperature and 2-D calculated temperature in tap-hole.

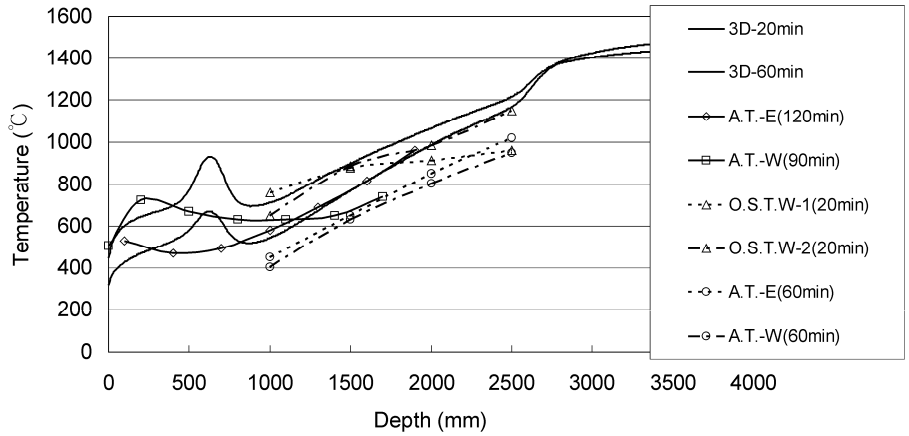

Fig. 9. Measured temperature and 3-D calculated temperature in tap-hole.

6. CONCLUSIONS

In this study, the heat transfer behavior of the sintered mud in the tap-hole area of No. 2 blast furnace at CSC has been analyzed and the calculated results can be summarized as below:

(1) A 2-D modified model was developed to investigate the influence of the properties of varied refractory and cooling systems on hearth temperature distribution. The thermal conductivity of mud-core plays an important role in tap-hole temperature distribution, but it is hard to define.

(2) To better simulate the tap-hole temperature profile, a 3-D simplified model was developed to and validated by measured data. The simulation result can get good agreement with measured data.
(3) The 3-D model can provide some information to site personnel for dealing with hot metal splashing and for the selection of new mud in the tap-hole.

REFERENCES

1. A. K. Vats and S. K. Dash: Ironmaking Steelmaking, 27 (2000), p. 123.
2. S. Dash, S. K Ajmani, A. Kumar and H. Sandhu: Ironmaking Steelmaking, 28 (2001), p. 110.
3. S. K. Dash, D. N. Jha, S. K. Ajmani and A. Upadhyaya: Ironmaking *Steelmaking Int. J. Technol. Adv.,* 31 (2004), p. 207.
4. Qinglin He, P. Zulli, F. Tanzil, B. LEE, J. Dunning and G. Evans: ISIJ International, 42 (2002), p. 235.
5. W. T. Cheng, C. N. Huang and S. W. Du: *Chem. Eng. Sci.,* 60 (2005), p. 4485. □